Available online at www.sciencedirect.com
SCIENCE DIRECT
Journal of the European Ceramic Society 26 (2006) 553–558
www.elsevier.com/locate/jeurceramsoc

Thermal residual stress gradients in an alumina–zirconia composite obtained by electrophoretic deposition

Mónica Popa [a,b], Pavol Hvizdos [c], Guy Anne [d], José M. Calderón-Moreno [a,*]

[a] *Departamento de Física Aplicada, Universidad Politécnica de Cataluña, Av. Canal Olimpic s/n, Castelldefels, Barcelona 08860, Spain*
[b] *Institute of Physical Chemistry "I. G. Murgulescu", Splaiul Independentei 202, Sector 6 77208, Bucharest, Romania*
[c] *Departamento de Materiales e Ingeniería Metalúrgica, Universidad Politécnica de Cataluña, Avda. Diagonal 647, Barcelona 08028, Spain*
[d] *Department of Metallurgy an Materials Engineering, Katholieke Universiteit Leuven, Spain*

Available online 10 August 2005

Abstract

In order to understand the mechanical behavior of layered composites with compositional gradient, it is necessary to determine their state of residual stresses. Compositionally graded materials can offer the advantage of eliminating abrupt changes in composition between layers having different thermal expansion coefficient. The existence of a compositional gradient can reduce discontinuities in thermal residual stresses, something beneficial from the point of view of the mechanical properties.

We present here a study of the microstructure and state of residual stressses in a layered material made of homogeneous layers of alumina and alumina–zirconia separated by thin (less than 300 μm) intermediate compositionally graded layers. The composite was obtained by controlled deposition of powders from solution using an electrophoretic deposition (EPD) method. The phase distribution and compositional gradient in the sintered composite were investigated using scanning electron microscopy (SEM). Thermal residual stresses generated during cooling after sintering were measured by using fluorescence ruby luminiscence piezo-spectroscopy and the profile of hydrostatic stress on alumina was determined at steps of about 300 μm along the direction of the compositional gradient, and at steps of about 30 μm in the compositionally graded layers. The obtained profile of hydrostatic stresses on alumina grains follows closely the profile of compositional changes along the layered composite. The presence of thin intermediate graded layers reduce significantly changes in stress in the layered composite.

Keywords: Al_2O_3; ZrO_2; Spectroscopy; Composites; Thermal residual stress

1. Introduction

The internal stresses caused by the elastic and thermal properties mismatch at an interface of two bulk materials can mitigate the successful implementation of layered composites. To address this problem, compositionally graded materials have been developed to satisfy the needs for properties that are unavailable in any single material and for graded properties to offset adverse effects of discontinuities. The introduction of gradual compositional changes removes large-scale interface-induced stress singularities and can even result in stress-free materials joints.[1,2] A wide variety of available processes have been reported for production of compositionally graded materials, such as plasma spraying, centrifugal casting, common powder metallurgy, PVD, CVD and colloidal processing. Electrophoretic deposition (EPD) is a fairly rapid low cost process, capable of producing continuously graded materials. EPD consists of two processes: the movement of charged particles in suspension in an electric field between two electrodes (electrophoresis) and particle deposition on one of the electrodes.[3] EPD allows the formation of plate-shaped binary functionally graded materials by depositing from a powder suspension to which a second suspension is continuously added during the process. The deposit is a close packed powder compact that needs sintering to achieve fully dense material components.

* Corresponding author.
E-mail address: jose.calderon@upc.es (J.M. Calderón-Moreno).

0955-2219/$ – see front matter © 2005 Elsevier Ltd. All rights reserved.
doi:10.1016/j.jeurceramsoc.2005.07.026

In order to understand the mechanical behavior, it is necessary to determine the state of residual stresses. In alumina containing composites, the position of the characteristic doublet in the luminiscence spectra from Cr^{3+} present in the alumina lattice, can be used to determine residual stresses.[4,5] The diameter of the exciting beam marks the limit to the lateral spatial resolution, allowing measurements at the desired microstructural feature in the size range from one micron to macroscopic regions. This technique have been used in alumina–zirconia composites, both a room temperature,[6–8] and at low temperatures.[9]

2. Experimental procedure

2.1. Sample preparation

The preparation and the indentation mechanical properties of the layered composite have been described previously.[10,11] The starting materials are 12 mol% CeO_2 co-precipitated ZrO_2 powder (Daiichi grade CEZ 12) with an average particle size of ~0.3 μm and Al_2O_3 powder (Baikowski grade SM8) with an average particle size of ~0.6 μm. As-received powders were ball-milled in ethanol for 24 h. Electrophoretic deposition (EPD) at constant voltage was performed after ultrasonication of freshly prepared suspensions of ball-milled powders with acetone and n-butylamine as suspension media, in a suspension flow-through deposition cell described previously, where a supply system add a second suspension to the circulating suspension in the mixing cell at a controlled rate.[10] The green bodies after EPD were sintered for 2 h at 1480 °C.

2.2. Scanning electron microscopy (SEM)

Surfaces of the layers were prepared for SEM by diamond polishing, thermal etching at 1400 °C for 1 h and finally Pt–Pd coated before observation, using a JEOL apparatus.

2.3. X-ray diffraction (XRD)

Powder X-ray diffraction patterns were obtained using Cu Kα radiation in a curved graphite-beam monochromator.

2.4. Raman

Raman spectra were recorded using the 547 nm excitation wavelength of an Ar^+ laser source equipped with a triple monochromator and a charge-coupled device (CCD) detector.

2.5. Luminiscence

The luminiscence spectra was measured using the blue and green lines, at 547 and 514.5 nm, respectively, of an Ar^+ laser equipped with a spectrometer T64000 with a triple monochromator and a CCD detector. Exposition times and laser power were 0.1–0.3 s and 500 mW, and the recorded spectral range from 686 to 701 nm, including the doublet characteristic of ruby luminiscence. An optical microscope and a movable *xy* sample stage were used to place the sample at successive 10 μm steps along the direction of the compositionally graded intermediate layer, perpendicular to the interfaces between the layers. The luminiscence spectra, with a laser beam diameter of 1–2 μm, were taken at each step along the line.

2.6. Calculation of residual stresses

The high purity alumina powder used for sample preparation was taken as internal reference as the "stress-free" position and its spectrum measured before and after each set of measurements. Observed peaks were fitted to a linear combination of Lorentzian and Gaussian and to a Voigt function using the Peakfit3 program; both fitting methods resulted in the same peak positions. The dependence between the hydrostatic stress, σ_h, 'seen' by the annalyzed alumina grains with the spectral shift of the ruby luminiscence R-line, compared to the stress-free position, $\Delta\lambda$, was first established by He and Clarke in polycrystalline alumina.[6] In our determinations of stress calculations we have used the peak of the doublet with higher wavenumber and the relationship:

$$\sigma_h \ (\text{MPa}) = 2760 \times \Delta\lambda \ (\text{nm}) \quad (1)$$

3. Results and discussion

SEM. Fig. 1 shows a polished and thermally etched cross-section of the composite, illustrating the compositional changes in the layered structure of the alumina–zirconia composite. There are three homogeneous and thicker layers, of alumina (left side in Fig. 1), alumina–20 vol.% zirconia (cen-

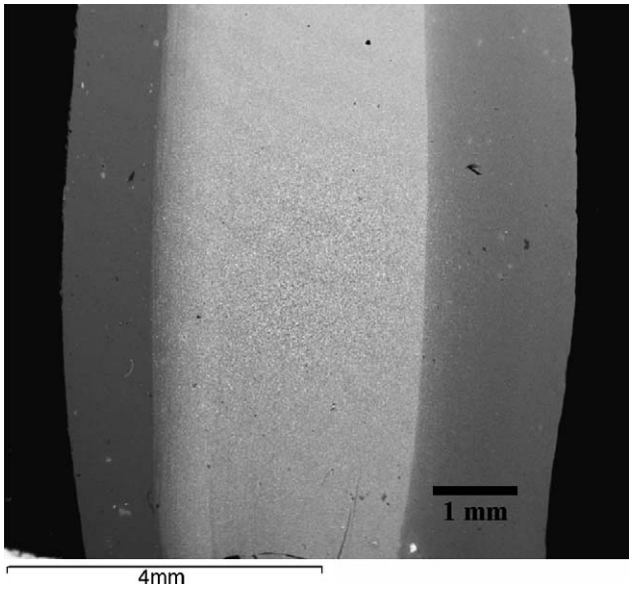

Fig. 1. SEM micrographs of a polished cross-section.

ter) and alumina–10 vol.% zirconia (right side), separated by thinner compositionally graded intermediate layers. The SEM micrographs of polished and thermally etched surfaces in Fig. 2 show the grain sizes and the distribution of both phases for the three homogeneous layers. Arrows in the micrograph showing the microstructure of the central layer show the presence of zirconia (bright grains) bigger grains, or agglomerates, in some cases with associated porosity. This can be deletereous for the mechanical stability of the composity, as we can expect higher thermal residual stress in the vicinity of zirconia agglomerates. It is also known that the martensitic transformation into the monoclinic phase of lower density, associated to the expansion of the zirconia grain and the subsequent creation of microcraking, is more likely to occur in bigger grains.[12] However, the XRD and Raman studies carried out did not detect the presence of monoclinic zirconia associated to the agglomerates.

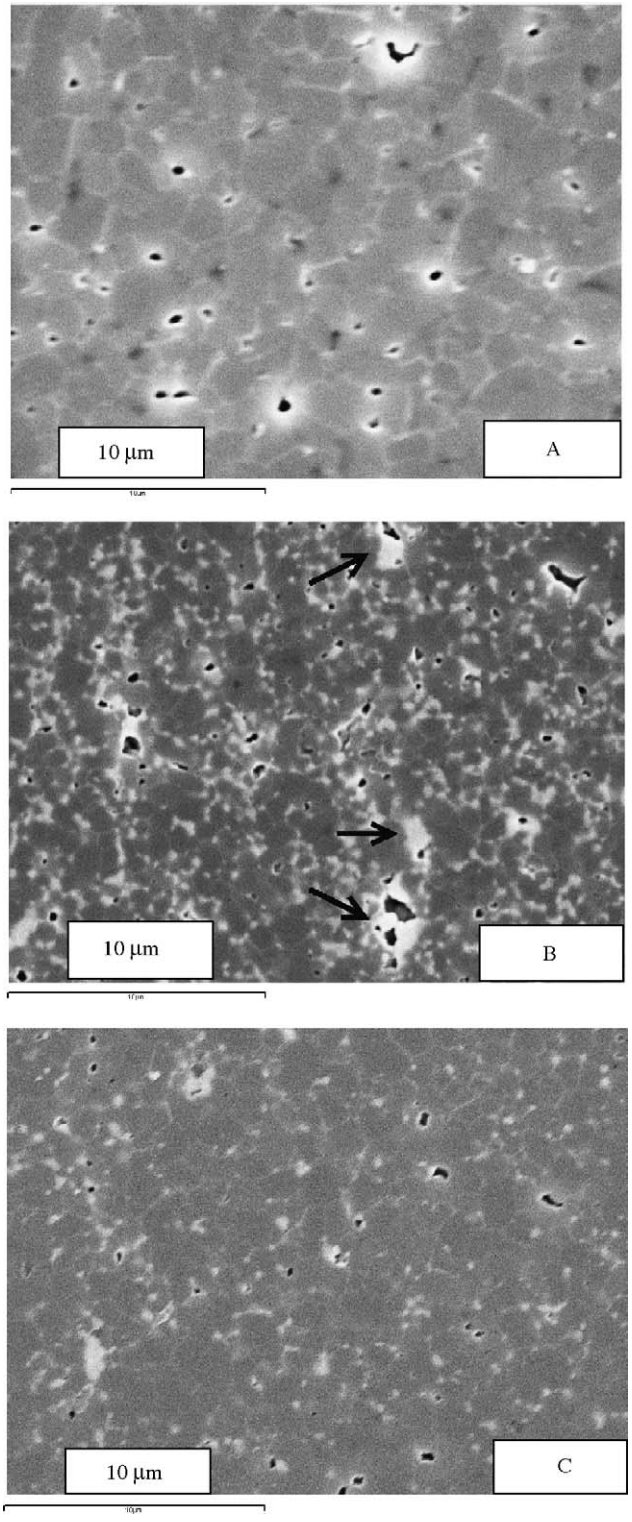

Fig. 2. SEM micrograph of polished and thermally etched surfaces of the alumina side (A), the alumina–zirconia homogeneous layers at the center (B) and the bottom side the composite (C).

3.1. XRD

Fig. 3 shows the spectra of the alumina side layer and the alumina–zirconia homogeneous layers at the opposite side and the center of the layered plate. In the alumina layer only the features of α-alumina (corundum) are observed. In the alumina–zirconia layer, corundum peaks and with less intensity tetragonal zirconia (t-Z) peaks are clearly detected. XRD detected only traces of the main monoclinic zirconia (m-ZrO_2) doublet (Fig. 4). We used the Eq. (2) to estimate the maximum volume fraction of m-ZrO_2 relative to tretragonal zirconia,

$$V_m = 1.6\frac{I_m}{(1.6I_m + I_t)}(< 1.7\%), \quad (2)$$

where I_m and I_t are the intensity of the peaks for m- and t-ZrO_2. The calculated volume fraction of monoclinic zirconia relative to total zirconia is less than 1.7%. This estimation means that the content of monoclinic zirconia in the central layer is less than 0.4 vol.%. For the calculation we did not eliminate background noise, because of the small signal at the sites of the main m-ZrO_2 doublet, where the signal

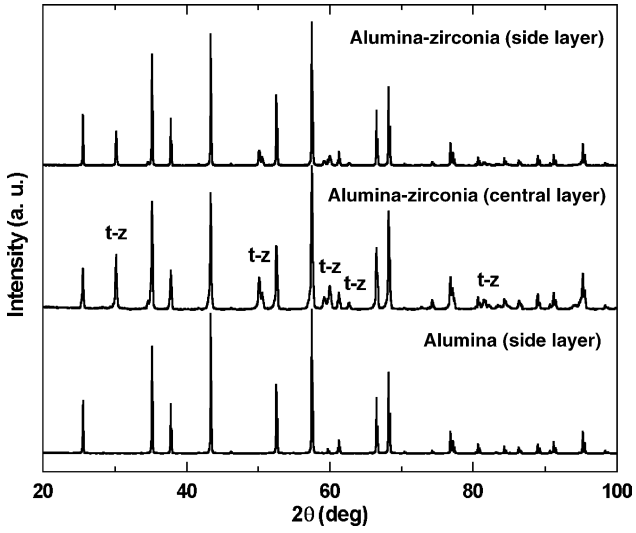

Fig. 3. XRD spectra at each side of the composite.

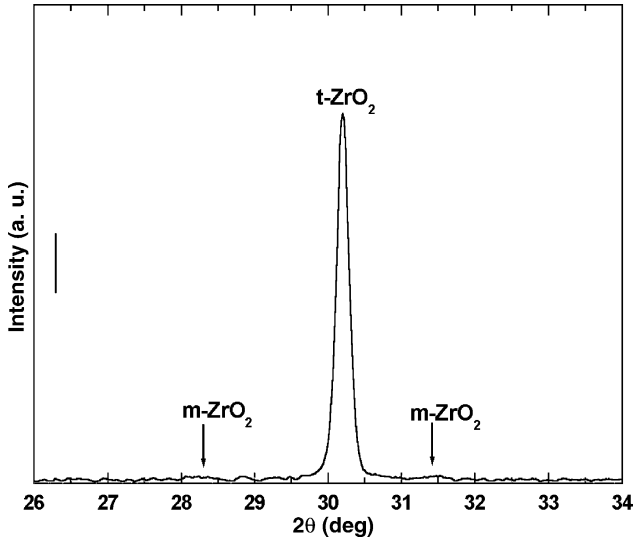

Fig. 4. XRD spectrum showing the region of the main tetragonal zirconia (t-ZrO_2) peak and monoclinic (m-ZrO_2) zirconia main doublet, for the central alumina–zirconia layer.

to noise ratio was less than 1. The given value is therefore an overestimation due to the resolution limit of our measurement.

3.2. Raman

Raman is a more powerful technique for the detection of zirconia allotropes.[13] Given the observation by SEM of the presence of zirconia agglomerates in the central layer, we used micro-Raman spectroscopy in order to determine the presence of monoclinic zirconia in the agglomerates. Measurements detected clearly the Raman features of tetragonal zirconia (t-ZrO_2) and α-Al_2O_3, while the features of other zirconia allotropes were not detected (Fig. 5). We can therefore conclude that the amount of monoclinic zirconia is not significant even in the agglomerates at the central layer with higher zirconia content.

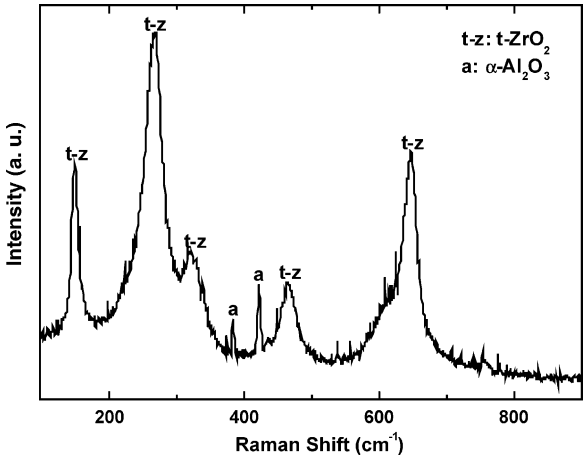

Fig. 5. Raman spectra of the two-phase layer.

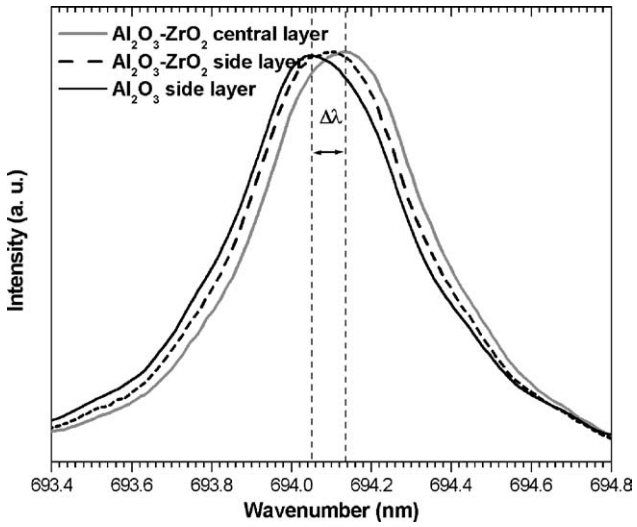

Fig. 6. Cr-luminiscence spectra for the higher wavenumber peak of the R-line luminiscence doublet.

3.3. Residual hydrostatic stress on alumina

Fig. 6 shows the Cr-luminiscence spectra taken in each of the three homogeneous alumina or alumina–zirconia layers. The spectral shift illustrated in Fig. 6 is associated to a significant change in the hydrostatic stress on the alumina grains at the different layers. The maximum spectral shift, between the center of the composite and the alumina side, is equivalent to a stress change of 230 ± 10 MPa, calculated using Eq. (1).

Fig. 7 shows the spatial evolution of the shift in wavelengths and the hydrostatic stress on alumina along the direction of the compositional gradients, taken at intervals of $\sim$300 μm. The graph of the peak position vs. distance have

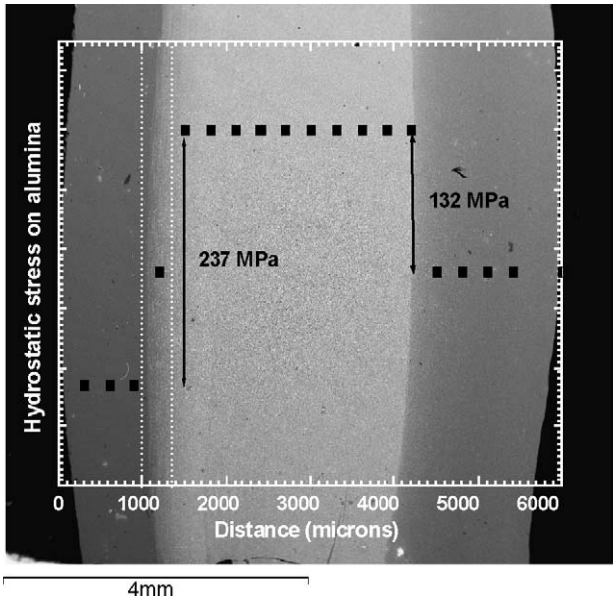

Fig. 7. Hydrostatic stress distribution along the layered composite.

been superimposed at the same scale on the SEM micrograph of Fig. 1, the cross-section along the direction of compositional changes, to illustrate clearly the correspondence between the different layers and the measured stresses. No change of residual stresses was detected away from the compositionally graded layers in any of the compositionally homogeneous layers. The region of stress changes is limited to the region with compositional changes. The profile of hydrostatic stresses, obtained from the spectral shifts measured using ruby fluorescence piezo-spectroscopy, follows closely the compositional gradient observed in the composite.

Regarding the stress distribution in the compositionally graded thin layers, we did new measurements at smaller intervals of 30 μm in the intermediate compositionally graded layers, the region delimited by dotted lines in Fig. 7, between the darker layer at the left and the brighter layer at the center. We did measurements at different points in the perpendicular line to the compositional gradient, with the same distance along the compositional gradient direction. The experimental points are taken at intervals of ∼30 μm. Fig. 8 shows the average values of hydrostatic stresses thus obtained, with the associated error bars showing the average stress scatter. The arrow in the central point illustrates the significant scattering of the measurements at that point, compared to the average scatter in the sample, shown as error bars.

First, the region of stress changes is ∼100–150 μm thick and, second, the intermediate graded layer showed a significantly higher scattering of residual stresses, compared to those obtained at the homogeneous thick layers (Fig. 8). The scattering is attributed to differences in the compositional gradient along the perpendicular to the gradient direction, as it was confirmed during SEM observations, thus they correspond to changes in the compositional gradient at different 'crossing lines' across the layer. The preparation of samples with less pronounced compositional gradient can reduce those local variations in the intermediate layers and the stress scatter.

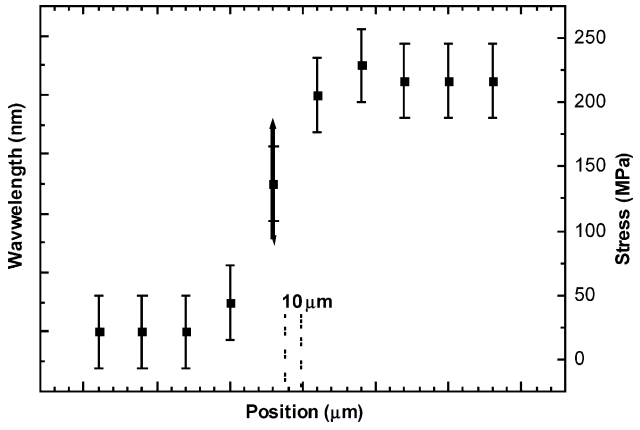

Fig. 8. Shift in wavelengths/hydrostatic streses along the compositionally graded layer.

4. Summary

The microstructure and state of residual stressses in a layered alumina–zirconia compositionally graded composite, obtained using an electrophoretic deposition method, were studied.

The profile of residual stresses measured by ruby luminiscence piezo-spectroscopy in the layered composite matched the compositional gradient observed by scanning electron microscopy. The hydrostatic stresses on alumina grains vary gradually according to the variation of composition in the compositionally graded layers.

Results indicate that the introduction of thin intermediate graded layers is a suitable method to reduce significantly changes in stress in the layered composite.

Acknowledgments

Work funded by CICYT, grant MAT2004-01214, and Generalitat de Catalunya grant 2001-SGR-00190.

References

1. Becker Jr., T. L., Cannon, R. M. and Ritchie, R. O., Statistical fracture modeling: crack path and fracture criteria with application to homogeneous and functionally graded materials. *Eng. Fract. Mech.*, 2002, **69**, 1521–1555.
2. Miyamoto, Y., Kaysser, W. A., Rabin, B. H., Kawasaki, A. and Ford, R. G., *Functionally Graded Materials: Design, Processing and Applications*. Kluwer Academic Publishers.
3. Put, S., Vleugels, J. and Van der Biest, O., Microstructural engineering of functionally graded materials by electrophoretic deposition. *J. Mat. Process. Tech.*, 2003, **143–144**, 572–577.
4. Ma, Q., Pompe, W., French, J. D. and Clarke, D. R., Residual stresses in Al_2O_3–ZrO_2 composites: a test of stochastic stress models. *Acta Met. Mat.*, 1994, **42**, 1673–1681.
5. He, J. and Clarke, D. R., Determination of the piezo-spectroscopic coefficients for chromium-doped sapphire. *J. Am. Ceram. Soc.*, 1995, **78**, 1347–1353.
6. Pezzotti, G., Sergo, V., Sbaizero, O., Muraki, N., Meriani, S. and Nishida, T., Strengthening contribution arising from residual stresses in Al_2O_3/ZrO_2 composites: a piezo-spectroscopy investigation. *J. Eur. Ceram. Soc.*, 1999, **19**, 247–253.
7. Gutierrez-Mora, F., Goretta, K. C., Majumdar, S., Routbort, J. L., Grimdisch, M. and Dominguez-Rodriguez, A., Influence of internal stresses in superplastic joining of zirconia toughened alumina. *Acta Mater.*, 2002, **50**, 3475–3486.
8. Popa, M., Calderón Moreno, J. M., Hvizdoš, P., Bermejo, R. and Anné, G., Residual stress profile determined by piezo-spectroscopy in alumina/alumina-zirconia layers separated by a compositionally graded intermediate layer. *Key Eng. Mat.*, 2005, **290**, 328–331.
9. Orera, V. M., Cemborlain, R., Merino, R. I., Peña, J. I. and Larrea, A., Piezospectroscopy at low temperatures: residual stresses in Al_2O_3–$ZrO_2(Y_2O_3)$ eutectics measured from 77 to 350 K. *Acta Mater.*, 2002, **50**, 4577–4686.
10. Vleugels, J., Anné, Put, S. and Van der Biest, O., Thick plate-shaped Al_2O_3/ZrO_2 composites with continuous gradient processed by electrophoretic deposition. *Functionally Graded Materials VII*. Trans Tech Publications, Switzerland, 2003, pp. 171–176.

11. Hvizdoš, P., Calderón Moreno, J. M., Ocenášek, J., Ceseracciu, L. and Anné, G., Mechanical properties of alumina/zirconia functionally graded material prepared by electrophoretic deposition. *Key Eng. Mat.*, 2005, **290**, 332–335.
12. Calderón-Moreno, J. M., de Arellano-López, A. R., Domínguez-Rodríguez, A. and Routbort, J. L., Microstructure and creep properties of alumina/zirconia ceramics. *J. Eur. Ceram. Soc.*, 1995, **15**, 983–988.
13. Kakihana, M., Yashima, M., Yohimura, M., Börjesson, L. and Kall, M., Application of Raman spectroscopy to phase characterization of ceramic high-Tc superconductors and zirconia related materials. *Trends Appl. Spectrosc.*, 1993, **1**.